In Silico Study of Aptamer Specificity for Detection of Insulin as Development for Diabetes Mellitus Diagnosis

Dinda Exelsa Mulyani, Iman Permana Maksum[*], and Muhammad Yusuf

Department of Chemistry, Faculty of Mathematics and Natural Sciences, Universitas Padjadjaran,
Jl. Raya Bandung-Sumedang km 21, Jatinangor 45363, Indonesia

Abstract: *Diabetes mellitus (DM) is a metabolic disorder characterized by elevated blood glucose levels. There are 2 types of DM where molecular-level diagnosis becomes very important because both have different treatments to avoid treatment errors. An electrochemical aptasensor as a type 2 DM detector with insulin target has been developed. This study aims to determine the interaction and specificity based on the values of RMSD, RMSF, and binding energy between aptamer and insulin when it reaches stability* in silico *compared to HbA1c and glucose. Docking simulations were performed on the HDOCK webserver and dynamics simulations for 1000 ns on the aptamer and protein molecular models used. The simulation results were analyzed to see the stability and visualized using VMD to see the conformation of the aptamer-ligand complex. The docking result showed higher binding energy between aptamer-insulin compared to other molecules, namely −221.87 kcal/mol. The results of RMSF and RMSD analysis of molecular dynamics simulations show that the system is stable, has the best binding energy value of −9.9510 kcal/mol. The aptamer complex with insulin showed better specificity compared to glucose and HbA1c based on RMSD, RMSF, and binding energy.*

Keywords: *diabetes mellitus; aptasensor; insulin*

■ INTRODUCTION

Diabetes mellitus (DM) is a degenerative disease caused by a prolonged increase in blood sugar due to dysfunction of secretion or insulin resistance [1]. According to International Diabetes Federation (IDF) in 2021, recorded deaths caused by DM are very high in Indonesia with a prevalence of 1 person every 5 s. This disease is closely related to premature morbidity and mortality which causes complications such as neuropathy, nephropathy, and retinopathy [2-4].

Commonly used diagnostics for DM are measuring blood sugar levels and HbA1c, but these diagnostics cannot distinguish the type of DM [5-7]. Therefore, there is a need for appropriate methods to overcome this problem. One of them is a diagnostic to determine the level of insulin in the blood so that treatment rationalization can be done appropriately. An increase in blood insulin levels is a marker in patients with type 2 DM who experience insulin resistance [7]. Insulin is a hormone that has an essential role in glucose metabolism. Insulin has 2 chains, namely chain A with 21 amino acids and chain B with 30 amino acids with a molecular weight of 5,802 g/mol and its isoelectric point at pH 5.5. Both chains are connected by 2 disulfide bonds from the N-helix of chain A to the center of B and the C-terminal from chain A to the center of chain B [8]. Variations in insulin levels are also a precursor to several degenerative disorders such as dyslipidemia, hypertension, and diabetes mellitus [9-10].

One of the interesting and widely studied methods for DM diagnostics is an electrochemical biosensor using aptamer as its bioreceptor commonly called aptasensor [11]. Aptamers are oligonucleotides or short pieces of single-stranded DNA/RNA molecules that can recognize specific target molecules. Aptamers were chosen because they have excellent characteristics as bioreceptors that have excellent affinity for biosensors as well as other applications, such as biomedical imaging,

targeted drug delivery, and biomarker discovery [12-13]. Research has been conducted on a transistor-based nanoelectronic aptasensor for HbA1c detection. Aptamer arrays were generated from the results of the systematic evolution of ligands by exponential enrichment (SELEX). Docking was carried out between the aptamer array and insulin binding site to determine the interaction and produced the best binding energy of −12.50 kcal/mol on hairpin 1 [14]. Furthermore, Mulyani et al. [15] have conducted electrochemical sensor research using ATP-binding aptamer to detect mitochondrial diabetes with the differential pulse voltammogram (DPV) method. The results of this study show excellent selectivity for aptamer against ATP compared to its analog, which is characterized by a significant increase in current peaks against measurements on ATP and aptamer, showing good specificity for ATP detection [16]. *In vivo* research on aptasensors for adenosine detection with direct monitoring of rat bodies has been conducted by Zhang et al. [17]. Their research showed that aptasensors can detect an increase in extracellular adenosine. Another research testing the use of aptasensors for diagnostic tools is the graphene multitransistor array aptasensor for dopamine detection as a diagnostic tool for brain disorders. The results showed that the aptasensor has a limit of detection of 1 aM (10^{-18} M) with dynamic detection ranges spanning 10 orders of magnitude up to 100 μM (10^{-8}), and a 22 mV/decade peak sensitivity in artificial cerebral spinal [18].

To complement DM diagnostics, an aptasensor that detects insulin as a marker of type 2 DM was developed [19-20]. Yoshida et al. [20] have selected aptamers that can bind insulin from DNA libraries by SELEX method, resulting in 3 aptamer sequences named IGA 1, IGA 2, and IGA 3. Furthermore, these 3 aptamer sequences were selected to determine the binding ability of aptamer, the result is IGA 3 has a higher affinity compared to insulin-linked polymorphic repeat region (ILPR). The aptamer array selected by Yoshida et al. was used by Kubo and Eguchi [19] for their research on electrochemical aptasensors immobilized on gold electrodes to determine their electrochemical activity measured by cyclic voltammetry. The results of this study indicate that the cathodic peak current of the IGA 3-hemin complex depends on insulin concentration. An *in vivo* study on the aptasensor for insulin detection was conducted, and the results showed that the aptasensor has a linear range between 1.0 pM–1.0 μM with a low detection limit (0.42 pM) [21].

Research has been conducted by Zhao et al. [22] on a dual signaling aptasensor for ultrasensitive detection of insulin to obtain a sensor with a high level of sensitivity and specificity. The specificity test of insulin aptasensor was conducted with thrombin, HSA, and HigG because they are considered as substances that interfere with the target during the detection process. The results showed that the specificity of the proposed aptasensor was very good for target detection. An aptasensor monitoring study for the detection of insulin using mesoporous silica nanoparticle thin films by electrochemically assisted self-assembly (EASA) method had a detection limit of 10–350 nM and showed good selectivity towards glucose, urea, glutathione, and dopamine [23]. However, the research on aptamers for insulin detection is still *in vitro* and *in vivo*, so it cannot provide information about the interaction and specificity between aptamer and target [22]. Therefore, it is necessary to conduct *in silico* research on the interaction and specificity of the aptamer to insulin compared to other proteins that can become impurities in the biosensor, namely HbA1c, and glucose, to increase the potential of the aptasensor as a type 2 DM diagnosis, which can then be applied as a molecular test in health facilities.

■ **EXPERIMENTAL SECTION**

Materials

The materials of this research are aptamer and insulin modeling, as well as other molecular structures, namely HbA1c and glucose, using several databases and software. Molecular interactions were studied based on molecular tethering and molecular dynamics using licensed or free access.

Instrumentation

The instrumentation of this research is a computer with OS Ubuntu 20.04.5 LTS, processor Intel Xeon(R)

CPU 5E-2689 0 @2.60GHz x 16, GPU NVIDIA Corporation3080, and 2.3 TB storage.

Procedure

Preparation of aptamer structure

The aptamer array used is entered into the mfold web server (https://bio.tools/mfold) to determine the folding that occurs and the 2D structure, then the aptamer array is entered into the 3DRNA/DNA webserver (http://biophy.hust.edu.cn/new/3dRNA) so that the 3D structure of the aptamer is obtained.

Preparation of insulin, Hb, HbA1c, GHSA, HSA and glucose structures

The protein structures of insulin and HbA1c were accessed and then retrieved from the database website Research Collaboratory for Structural Bioinformatics (RCSB) Protein Data Bank (PDB) at https://www.rcsb.org/ with PDB ID codes 6X4X and 3B75. After that, the target protein structure was remodeled. The protein part was modeled using the Modeler program, while the glucose was obtained from the webserver https://pubchem.ncbi.nlm.nih.gov/. The obtained structures were saved in .pdb file format.

Docking simulation

The results of the 3D structure model of ssDNA aptamer and 3D structure of insulin in .pdb format were entered into HDOCK software. After that, it was submitted so that the aptamer-insulin complex obtained docking results in .pdb format and binding affinity data in kcal/mol. The validity of the docking method is determined by assessing the root mean square deviation (RMSD) value, with a value of $\leq 2\,\text{Å}$ considered acceptable. The same procedure was carried out for insulin where insulin was replaced with other target molecules, namely HbA1c or glucose, to be compared with the insulin-aptamer results.

Molecular dynamis simulation

After the docking simulation, the complex coordinates were saved in a .pdb file and entered into the Amber20 molecular dynamics simulation system. The simulation was run for 1000 ns. Force fields were used, including DNA.OL15 for the aptamer, protein.ff14SB for the protein receptor, and gaff2 for glucose. The stages

performed were minimization, heating, equilibration, and production. After that, the resulting output is analyzed. Some of the analyses include RMSD, RMSF, hydrogen bonding, and VMD visualization. The same procedure was carried out for insulin where insulin was replaced with other target molecules, namely HbA1c or glucose, and then the results of the insulin-aptamer complex were compared.

■ RESULTS AND DISCUSSION

In this study, the ssDNA aptamer IGA 3 sequence [5'-GGT GGT GGG GGG GGT TGG TAG GGT GTT TTC-3'] with a sequence length of 30 bp was used. The aptamer structure is not yet in the database, so the 3D structure of the aptamer is made using the 3DRNA web server by entering the aptamer sequence so that several 3D structure options are generated from the IGA 3 aptamer sequence, and the best one is selected (Fig. 1). The aptamer structure obtained was hybridized based on Watson-Crick base pairs. In Watson-Crick base pairing, adenine (A) forms a base pair with thymine (T), while guanine (G) with cytosine (C) in DNA. In RNA, thymine (T) is replaced by uracil (U).

Target molecules were downloaded from the RCSB PDB website database with PDB IDs, including insulin (ID: 6X4X), HbA1c (ID: 3B75), and glucose structure obtained from Pubchem database with CID code 5793. Furthermore, each protein structure was remodeled using Modeler to ensure that there were no missing amino acid sequences and to obtain data with good accuracy. In addition, insulin and HbA1c structures were created by removing water molecules and adding hydrogen. Ramachandran plot analysis was performed to ensure the quality of the protein model. This plot depicts the presence of amino acid residues to assess the
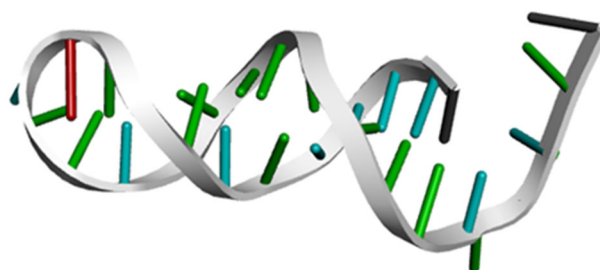
Fig 1. 3D structure modeling results of IGA 3 aptamer

stereochemical quality of the protein model structure. The model is said to be good if the percentage of residues in the allowed region is more than 90% [24]. The insulin model has 100% residues located in the allowed region and the HbA1c model has 94.3% residues in the allowed region so the model can be said to be good. The modeling results are depicted in Fig. 2. Furthermore, the structure was improved by removing water molecules and adding hydrogen before being inserted into the docking simulation.

Aptamer structures and molecules that have been prepared and inputted into the docking system on HDOCK. The docking method was validated first

between the aptamer and insulin, obtaining an RMSD value of 0.78 Å from the validation results. The RMSD value is less than 2 Å, so the method is acceptable. Next, docking was carried out between the aptamer and HbA1c and glucose. From the docking results that have been done (Fig. 3), we obtained information in the form of binding affinity value between aptamer and target as well as the interaction that occurs. The binding affinity value data is then summarized in Table 1 along with the interactions that occur. The binding energy value between the aptamer-insulin complex is −221.87 kcal/mol, providing a superior binding energy value compared to HbA1c and glucose.
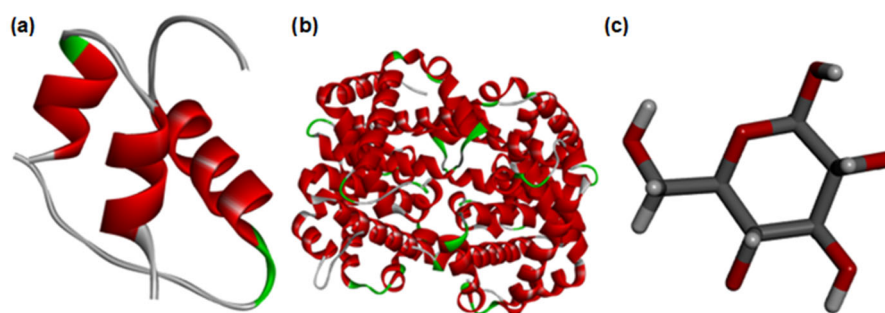
Fig 2. Target protein and glucose structures from preparation and homology modeling (a) insulin, (b) HbA1c, and (c) glucose
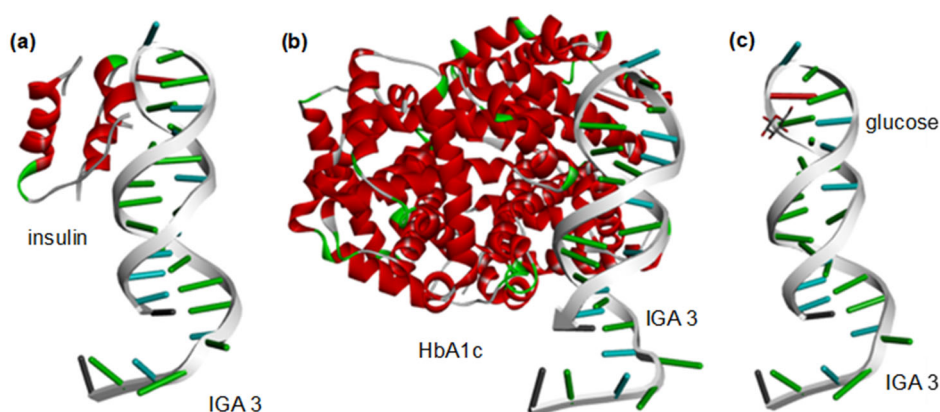
Fig 3. 3D visualization of aptamer docking results with the target: (a) aptamer complex with insulin, (b) aptamer complex with HbA1c, and (c) aptamer complex with glucose

Table 1. Binding affinity values and interactions that occur between aptamers with several molecules are sorted by binding affinity value from large to small

	Target	Binding affinity (kcal/mol)	Interactions
	Insulin	−221.87	G13, G18, G21, and G22
Aptamer IGA 3	HbA1c	−204.46	G9, G10, G11, G13, G18, and G22
	Glucose	−85.54	G17

From the docking results, it can be seen that the guanine base makes a very large contribution to the interaction (Fig. 4). From its structure, it also contains adjacent polyguanines that can form a G-quadruplex that confines the ligand with a fairly strong interactions seen from the binding energy [3-4]. However, at the docking stage, the conformational stability could not be confirmed, so we proceeded to molecular dynamics simulation.

The docking simulation results were then saved in .pdb format to be imported into the molecular dynamics simulation system using the Amber20 program. Simulations were carried out to determine the stability and specificity formed between aptamer and insulin compared to other inhibitor proteins. The aptamer molecule was separated from insulin and saved with a .pdb file, and then the two molecules were adjusted using pdb4amber. After the molecules have been adjusted, they are entered into the Leap feature to be combined and given a force field. The force fields used are leaprc.DNA.OL15 for aptamer, leaprc.ff14SB for insulin, and leaprc.tip3p for waterbox. Molecular dynamics simulation was carried out with minimization, heating, equilibrium, and production stages for 1000 ns. The analysis parameters reviewed were RMSD, RMSF, hydrogen bonding, and binding energy. Furthermore, the results of the RMSD analysis show the movement that occurs between insulin-aptamer complex, and the more stable the graph indicates the stability of the complex formed. The RMSF value shows the extent to which each aptamer residue moves. Visualization using VMD before and after simulation results are shown in Fig. 5.

The results of the RMSD analysis that occurs between aptamer and insulin show slight fluctuations with the RMSD value of insulin, which is around 12–19 Å, while the value for aptamer RMSD has good stability where the value range is between 3–6 Å which indicates that the molecule does not move freely and has reached a stable position to bind to insulin (Fig. 6). This is validated from the visualization of simulations using VMD, where at the beginning of the simulation aptamer and insulin experience movement indicated by the increasing RMSD value.

The results of RMSF analysis that occurred during the simulation on the insulin-aptamer complex showed that there were four increases in distance changes compared to other residues, namely residues T14, T19, G22, and T26. The increase in residues can be considered as the binding pocket side of insulin because the increase in fluctuations indicates that the residue is more flexible than the residues next to it (Fig. 7).

Analysis of hydrogen bonds taken are hydrogen bonds that have a percentage of presence of about 10% or above because it is considered quite significant in a simulation. Insulin aptamer complex bonding shows that there are several hydrogen bond interactions. Based on the data in Table 2 shows that the majority of bonds occur in thymine and guanine, where binding occurs to
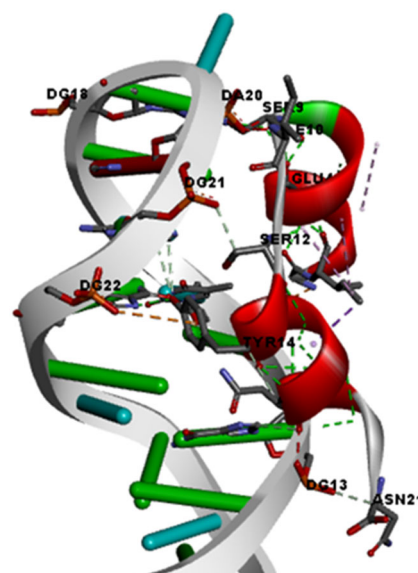
Fig 4. 3D visualization of the interaction between the aptamer and insulin after docking
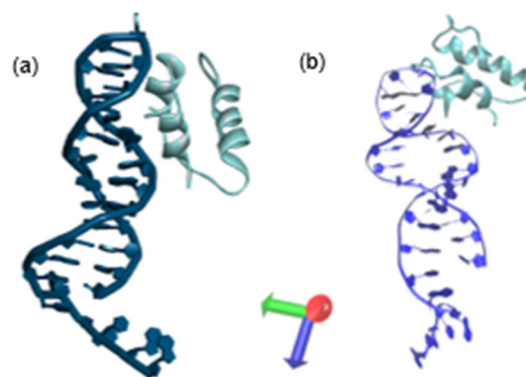
Fig 5. Conformation of insulin-aptamer (a) before and (b) after simulation for 1000 ns
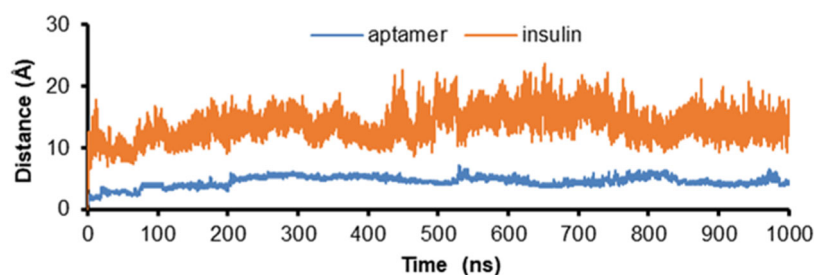
Fig 6. RMSD graph for 1000 ns on aptamer and insulin complex. The graph of aptamer (blue) and insulin (orange), shows that there is a stable complex between aptamer and insulin
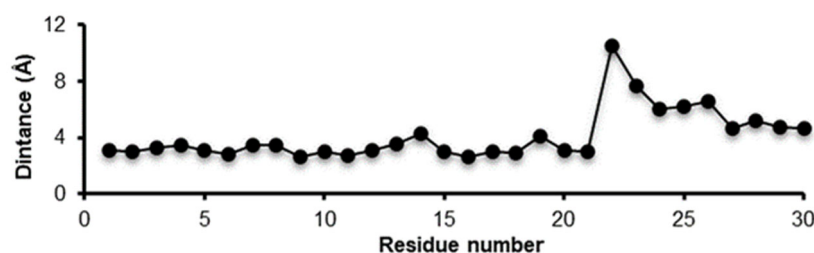
Fig 7. RMSF graph of the aptamer. The graph shows movement at residues T14, T19, G22, and T26, presumably the four residues are the binding pocket of insulin

Table 2. Hydrogen bonding of the insulin-aptamer complex

#Acceptor	Donor H	Donor	Frames	Fraction	Average distance (Å)	Average angle (°)
DA_20@OP2	SER_32@HG	SER_32@OG	22994	0.4599	26.777	1.642.302
SER_39@OG	DT_19@H3	DT_19@N3	19214	0.3843	28.752	1.610.113
DG_13@OP2	ASN_51@HD22	ASN_51@ND2	18795	0.3759	28.423	1.631.880
DT_19@O4	ILE_40@H	ILE_40@N	17435	0.3487	28.770	1.578.361
GLU_47@OE1	ARG_73@HH21	ARG_73@NH2	13684	0.2737	27.945	1.578.597
DG_18@O6	SER_39@HG	SER_39@OG	13143	0.2629	27.424	1.594.266
GLU_47@OE2	ARG_73@HH21	ARG_73@NH2	13073	0.2615	27.971	1.572.153
GLU_34@OE2	THR_81@H	THR_81@N	11973	0.2395	28.436	1.595.432
DG_14@OP2	ASN_51@HD21	ASN_51@ND2	10653	0.2131	28.315	1.610.714
GLU_47@OE2	ARG_73@HE	ARG_73@NE	10218	0.2044	28.320	1.563.959
CYX_41@O	LEU_57@H	LEU_57@N	9274	0.1855	28.511	1.597.139
GLU_47@OE1	ARG_73@HE	ARG_73@NE	9002	0.1800	28.352	1.561.492
DT_19@O2	GLN_45@HE22	GLN_45@NE2	8943	0.1789	28.453	1.604.252
GLU_34@OE1	THR_81@H	THR_81@N	8606	0.1721	28.415	1.587.075
DT_15@O4	ASN_48@HD21	ASN_48@ND2	7645	0.1529	28.603	1.586.181
PHE_76@O	TYR_49@HH	TYR_49@OH	7306	0.1461	27.619	1.643.622
DT_156@O4	GLN_45@HE22	GLN_45@NE2	7046	0.1409	28.552	1.614.602
DT_15@OP2	GLN_35@HE21	GLN_35@NE2	6997	0.1399	28.181	1.617.713
ASN_51@O	ARG_73@HH22	ARG_73@NH2	6834	0.1367	27.924	1.559.490
DT_16@O4	GLN_35@HE22	GLN_35@NE2	5737	0.1147	28.555	1.590.156
DG_12@OP1	ASN_51@HD21	ASN_51@ND2	5460	0.1092	28.842	1.631.600
DG_18@O6	ILE_40@H	ILE_40@N	5394	0.1079	28.536	1.565.951
ILE_40@O	DG_18@H1	DG_18@N1	5392	0.1078	28.684	1.565.483

to oxygen atoms (O) on phosphates or O atoms in ribose sugars, and specifically for guanine there is a bond to oxygen derived from guanine bases.

The same treatment was carried out on the molecular dynamics simulation between the aptamer and other molecules (HbA1c and glucose) to determine the specificity of the aptamer to insulin. All simulations were performed with the same input and treatment as before. The visualization results of the simulation are shown in Fig. 8.

RMSD values from the simulation results between aptamers and several molecules show a good level of specificity for the insulin-aptamer complex compared to the HbA1c-aptamer complex and glucose-aptamer complex. In the insulin-aptamer complex, the RMSD value of insulin is between the range of 12–19 Å and aptamer in the range of 3–6 Å. As for the HbA1c-aptamer complex, the RMSD value of aptamer is in the range of 11–16 Å, and for HbA1c shows high fluctuations in the range of 0–400 ns. There are slight fluctuations in the range of 400–1000 ns, namely changes in the distance in the range of 42–50 Å. The glucose-aptamer complex showed slight fluctuations in the aptamer in the range of 6–10 Å for glucose, experiencing very high fluctuations from the beginning of the simulation to the end of the simulation in the range of 2–80 Å. Visualization of the trajectory of the simulation results of the insulin-aptamer complex for 1000 ns tends to experience a slight change in position in the form of vibration of each atom to maintain the best position to bind to each other, while the visualization of the trajectory for the HbA1c-aptamer complex shows that there is a change in the shape of the structure of HbA1c at the beginning of the simulation where the protein undergoes a split sub unit so that the HbA1c structure is divided into two parts and in the movement after 400 ns the aptamer with the new HbA1c maintains its position so that at the beginning of the simulation until 400 ns the complex experiences a very high distance change and fluctuates, and for the trajectory results of simulation results for the glucose-aptamer complex showing the movement of glucose, it can be seen that the displacement/movement of the ligand still occurs and does not experience position stability indicated by the value which is still quite fluctuating from the beginning to the end of the simulation (Fig. 9).

Comparison of RMSF values between aptamers with insulin, HbA1c, or glucose is located on the residue number that has fluctuations that are considered as the binding side of the target. For aptamer has four alleged binding sides namely at 14, 19, 21, and 26, while for HbA1c has three alleged binding sides namely residue numbers 5, 18, and 24, and glucose at residue number 18 (Fig. 10). The analysis of hydrogen bonds for the HbA1c aptamer complex shows the same as insulin, namely, the majority of bonds occur on O atoms from phosphates,
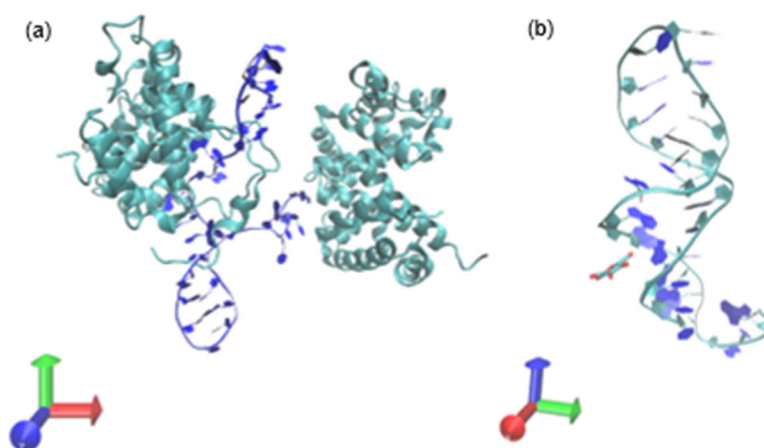
Fig 8. Visualization of simulation results for 1000 ns: (a) HbA1c aptamer complex and (b) glucose aptamer complex after simulation
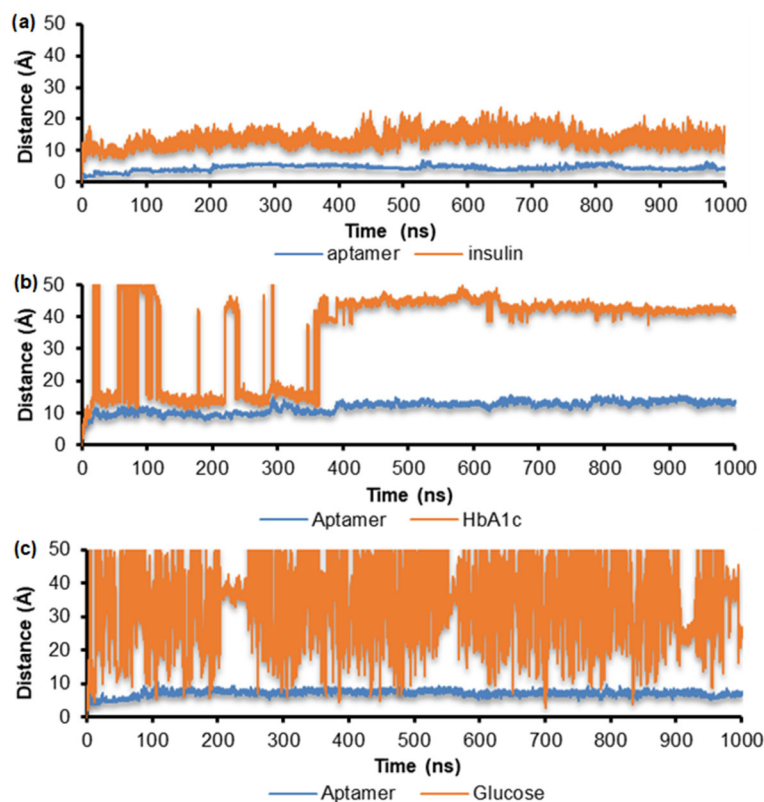
Fig 9. Comparison of RMSD of the three complexes for 1000 ns: RMSD analysis of (a) insulin-aptamer complex, (b) HbA1c-aptamer complex, and (c) glucose-aptamer complex
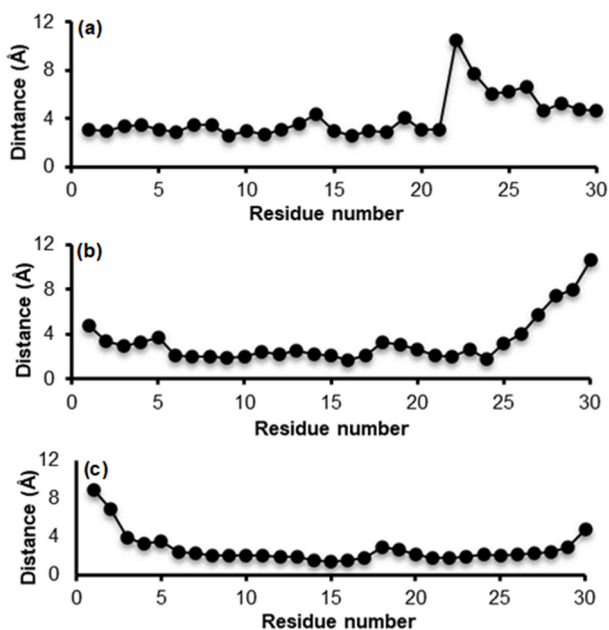
Fig 10. Comparison of RMSF of the three complexes for 1000 ns: (a) insulin aptamer complex, (b) HbA1c aptamer complex, and (c) glucose aptamer complex

sugar groups, or nitrogenous bases. But for sugar complexes, there are no hydrogen bonds that have a percentage of 10% or more, this is in accordance with the simulation situation where glucose does not reach stable interactions.

The next analysis is the binding energy between the aptamer and insulin. Binding energy is used as a parameter to determine the stability of a complex. When the binding energy value is lower (−), then the negative sign indicates that the reaction takes place exotherm (releasing energy) and vice versa. When the symbol is positive it indicates that the interaction is endotherm (using energy). Therefore, the energy that gives a negative sign indicates that the interaction is easily formed (favorable) and stable. The data in Table 3 shows that the insulin aptamer complex has better binding energy, followed by glucose and finally HbA1c. This can be caused by the calculation of complex components that involve the calculation of binding between the receptor

Table 3. The energy of the simulation system

	Complex aptamer insulin	Complex aptamer HbA1c	Complex aptamer glucose
	Energy total (kcal/mol)		
Complex	−6,316.7804	−11,196.4109	−5,067.6564
Receptor	−5,125.1993	−4,621.8897	−5,093.2030
Ligand	−1,181.6301	−6,973.7168	26.3648
Binding Energy	−9.9510	399.1956	-0.8181

and ligand, where HbA1c requires considerable energy to split its molecules so that it requires higher energy to bind (unfavorable).

CONCLUSION

Aptamer interacts with insulin in the simulation for 1000 ns. Based on the RMSD and RMSF profiles, the values are stable at 100–1000 ns, indicating that the stability of the resulting complex is quite good. Significant interactions occurred in nine hydrogen bonds, respectively, between insulin and A20, T19, G13, G18, G14, T15, T16, G12, and G18 on the aptamer. Specifically, the insulin aptamer complex has good specificity compared to HbA1c and glucose. Based on the binding energy value of insulin is better at −9.9510 kcal/mol than HbA1c or glucose, supported by the RMSD and RMSF data, insulin shows fluctuating stability while HbA1c and glucose show fluctuating values against the ligand and that indicates the complex is not yet stable.

ACKNOWLEDGMENTS

CONFLICT OF INTEREST

The authors declare no conflict of interest.

AUTHOR CONTRIBUTIONS

Iman Permana Maksum and Dinda Exelsa Mulyani performed data preparation. Iman Permana Maksum, Dinda Exelsa Mulyani, and Muhammad Yusuf conceived and designed the experiments. Dinda Exelsa Mulyani and Muhammad Yusuf performed all computational experiments. Iman Permana Maksum, Muhammad Yusuf, and Dinda Exelsa Mulyani analyzed the results. Dinda Exelsa Mulyani revised and edited the manuscript. All authors have read and agreed to the published version of the manuscript.

REFERENCES

[1] Liu, S., Shen, Z., Deng, L., and Liu, G., 2022, Smartphone assisted portable biochip for non-invasive simultaneous monitoring of glucose and insulin towards precise diagnosis of prediabetes/diabetes, *Biosens. Bioelectron.*, 209, 114251.

[2] International Diabetes Federation, 2021, *IDF Diabetes Atlas*, 10th Ed., International Diabetes Federation, Brussels, Belgium.

[3] Kahanovitz, L., Sluss, P.M., and Russell, S.J., 2017, Type 1 diabetes - A clinical perspective, *Point Care*, 16 (1), 37–40.

[4] Zaccardi, F., Webb, D.R., Yates, T., and Davies, M.J., 2016, Pathophysiology of type 1 and type 2 diabetes mellitus: A 90-year perspective, *Postgrad. Med. J.*, 92 (1084), 63–69.

[5] Priatna, A.S., Fadil, R.M.R., and Susanto, N.H., 2017, Blood glucose level and HbA1C in pediatric patients with diabetes mellitus type 1, *Althea Med. J.*, 4 (2), 217–220.

[6] American Diabetes Association Professional Practice Committee, 2021, Classification and diagnosis of diabetes: Standards of medical care in diabetes-2022, *Diabetes Care*, 45 (Suppl. 1), S17–S38.

[7] International Expert Committee, 2009, International expert committee report on the role of the A1C assay in the diagnosis of diabetes, *Diabetes Care*, 32 (7), 1327–1334.

[8] Fargion, S., Dongiovanni, P., Guzzo, A., Colombo, S., Valenti, L., and Fracanzani, A.L., 2005, Iron and

insulin resistance, *Aliment. Pharmacol. Ther.*, 22 (S2), 61–63.

[9] Luong, A.D., Roy, I., Malhotra, B.D., and Luong, J.H.T., 2021, Analytical and biosensing platforms for insulin: A review, *Sens. Actuators Rep.*, 3, 100028.

[10] Gorai, B., and Vashisth, H., 2022, Progress in simulation studies of insulin structure and function, *Front. Endocrinol.*, 13, 908724.

[11] Radi, A.E., and Abd-Ellatief, M.R., 2021, Electrochemical aptasensors: Current status and future perspectives, *Diagnostics*, 11 (1), 104.

[12] Villalonga, A., Pérez-Calabuig, A.M., and Villalonga, R., 2020, Electrochemical biosensors based on nucleic acid aptamers, *Anal. Bioanal. Chem.*, 412 (1), 55–72.

[13] Mulyani, D.E., and Maksum, I.P., 2023, Detection of biomarker using aptasensors to determine the type of diabetes, *Diagnostics*, 13 (12), 2035.

[14] Anand, A., Chen, C.Y., Chen, T.H., Liu, Y.C., Sheu, S.Y., and Chen, Y.T., 2021, Detecting glycated hemoglobin in human blood samples using a transistor-based nanoelectronic aptasensor, *Nano Today*, 41, 101294.

[15] Mulyani, R., Yumna, N., Maksum, I.P., Subroto, T., and Hartati, Y.W., 2022, Optimization of aptamer-based electrochemical biosensor for ATP detection using screen-printed carbon electrode/gold nanoparticles (SPCE/AuNP), *Indones. J. Chem.*, 22 (5), 1256–1268.

[16] Rustaman, R., Rafi Rahmawan, R., and Maksum, I.P., 2023, *In silico* study of aptamer specificity for detection of adenosine triphosphate (ATP) as biosensor development for mitochondria diabetes diagnosis, *Turk. Comput. Theor. Chem.*, 7 (2), 58–69.

[17] Zhang, D., Ma, J., Meng, X., Xu, Z., Zhang, J., Fang, Y., and Guo, Y., 2019, Electrochemical aptamer-based microsensor for real-time monitoring of adenosine *in vivo*, *Anal. Chim. Acta*, 1076, 55–63.

[18] Abrantes, M., Rodrigues, D., Domingues, T., Nemala, S.S., Monteiro, P., Borme, J., Alpuim, P., and Jacinto, L., 2022, Ultrasensitive dopamine detection with graphene aptasensor multitransistor arrays, *J. Nanobiotechnol.*, 20 (1), 495.

[19] Kubo, I., and Eguchi, T., 2015, Study on electrochemical insulin sensing utilizing a DNA aptamer-immobilized gold electrode, *Materials*, 8 (8), 4710–4719.

[20] Yoshida, W., Mochizuki, E., Takase, M., Hasegawa, H., Morita, Y., Yamazaki, H., Sode, K., and Ikebukuro, K., 2009, Selection of DNA aptamers against insulin and construction of an aptameric enzyme subunit for insulin sensing, *Biosens. Bioelectron.*, 24 (5), 1116–1120.

[21] Zeng, X., Wang, H., Zeng, Y., Yang, Y., Zhang, Z., and Li, L., 2023, Label-free aptasensor for the ultrasensitive detection of insulin via a synergistic fluorescent turn-on strategy based on G-quadruplex and AIEgens, *J. Fluoresc.*, 33 (3), 955–963.

[22] Zhao, M., Liao, L., Wu, M., Lin, Y., Xiao, X., and Nie, C., 2012, Double-receptor sandwich supramolecule sensing method for the determination of ATP based on uranyl–salophen complex and aptamer, *Biosens. Bioelectron.*, 34 (1), 106–111.

[23] Asadpour, F., Mazloum-Ardakani, M., Hoseynidokht, F., and Moshtaghioun, S.M., 2021, *In situ* monitoring of gating approach on mesoporous silica nanoparticles thin-film generated by the EASA method for electrochemical detection of insulin, *Biosens. Bioelectron.*, 180, 113124.

[24] Pertiwi, W., Muharram, L.H., and Maulana, F.A., 2022, Prediksi struktur 3D L-asparaginase bakteri laut *Vibrio* sp. AND4 dengan metode homology modelling, *JSFK*, 9 (2), 121–128.